

Boosting to identify: pseudoscalar searches with di-leptonic tops

Dorival Gonçalves^{1,*} and David López-Val^{2,†}

¹*Institute for Particle Physics Phenomenology, Department of Physics, Durham University, United Kingdom*

²*Centre for Cosmology, Particle Physics & Phenomenology CP3, Université catholique de Louvain, Belgium*

The quest for new heavy states is a critical component of the LHC physics program. In this letter, we study the search for pseudoscalar bosons produced in association with a $t\bar{t}$ pair. We consider the final state $t\bar{t}A \rightarrow t\bar{t}b\bar{b}$ with di-leptonic top pair signature, and reconstruct the boosted $A \rightarrow b\bar{b}$ candidate with jet substructure techniques, achieving a remarkable sensitivity over a broad range of pseudoscalar masses and Yukawa couplings. We apply this strategy to a Type-I Two-Higgs-Doublet Model, demonstrating its ability to probe a realistic, UV-complete extended Higgs sector. In particular, we find that the 13 TeV LHC with 300 fb^{-1} of data can constrain the region $\tan\beta > 1.5$ at 95% CL for a light pseudoscalar with $m_A = 50$ GeV. Moreover, the whole mass range $20 \text{ GeV} < m_A < 210 \text{ GeV}$ can be ruled out for $\tan\beta \leq 1$. Finally, we show that it is also possible to directly probe the CP-structure of the heavy scalar, and hence to distinguish a CP-odd (A) from a CP-even (H) 2HDM resonance.

CONTENTS

I. Introduction	1
II. Analysis	2
III. A BSM scenario	4
A. Extended Higgs sector	4
B. Parameter space	5
IV. CP measurement: $t\bar{t}A$ vs. $t\bar{t}H$	7
V. Summary	8
References	8

I. INTRODUCTION

Many of the fundamental questions brought to the fore by the Higgs-like 125 GeV discovery [1] remain as of today unanswered. A primordial one is whether the observed resonance does in fact account for electroweak symmetry breaking and mass generation in exactly the form postulated by Higgs, Englert and Brout [2–4]. Or if it is rather a first footstep into the Beyond: namely, the vast new physics territory in which the 125 GeV particle would be part of an extended Higgs sector, possibly within the reach of the LHC. Notwithstanding, the great agreement between a pure SM-like Higgs hypothesis and the experimental data implies that, if actually around, additional Higgs partners can only mildly mix with the 125 GeV state, and thus have a likely unmeasurable impact on its properties [5].

Direct scalar searches, for instance through heavy quark-rich final states [6–13], are therefore a paramount

avenue towards an extended Higgs sector. Among the possible candidates, a relatively light pseudoscalar A is not yet overly constrained, and may lie even in the few GeV range. Such mild bounds reflect in part that the A state cannot couple at tree level to the SM vector bosons, but only through loop effects [14]. In addition, the overwhelming SM backgrounds render fermionic decays signatures troublesome to tackle. An emblematic case is the process $pp(gg) \rightarrow A + \text{jets}$ where, in spite of the possibly large rates, the $A \rightarrow b\bar{b}$ mode is experimentally inaccessible. One way around the challenging QCD environment has been identified, e.g., for the SM Higgs associated production along with leptons in the channels Zh [15] and $t\bar{t}h$ [16, 17]. With the use of jet substructure techniques, both channels can help to access the dominant, yet challenging, decay mode $h \rightarrow b\bar{b}$. Likewise, heavy quark-rich final states could be operative to pin down pseudoscalar states through $A \rightarrow b\bar{b}$, and also $t\bar{t}A$ with fully leptonic top-quark decays.

In addition to setting bounds on the pseudoscalar mass-coupling strength plane, these decay modes also grant direct access to the CP-structure of the new state through the spin correlations analysis [17]. A direct separation between the CP-even (H) from the CP-odd (A) hypotheses would be a primary task following an eventual signal excess. As a matter of fact, typical multi-Higgs extensions, such as the Two-Higgs-Doublet Model (2HDM), include both types of bosons, with rather similar collider footprints in the scenarios best compatible with the current data.

Our aim in this letter is to cover a wide range of masses up to $m_A \sim 2m_t$ in a pseudoscalar search through the usually dominant channel $A \rightarrow b\bar{b}$, where the CP-odd state is produced through the $t\bar{t}A$ mode with di-leptonic tops, and jet substructure techniques are exploited to reconstruct the resonance candidate. Similarly to Refs. [12, 13], our starting logics is to simulate our signal with a Simplified Model. We show the power of this analysis to significantly constrain the parameter space of a Simplified Model, by adapting the jet substructure

* dorival.goncalves@durham.ac.uk

† david.lopezval@uclouvain.be

ture tagging for different mass regimes. We find competitive sensitivities, most significantly for pseudoscalar mass and Yukawa coupling ranges which are arduous to access otherwise. Next, we examine the implications of this search on the *alignment without decoupling* limit of the 2HDM. So doing, we assess the ability of the $t\bar{t}A(b\bar{b})$ analysis to probe realistic scenarios of a UV-complete extended Higgs sector. Lastly, we show that this channel also grants direct access to the CP-structure of such a hypothetical novel resonance.

This paper is organised as follows. In Section II we provide the details of the signal and background simulation and the boosted $A \rightarrow b\bar{b}$ reconstruction, illustrating the results of our collider analysis in the Simplified Model setup. The corresponding interpretation in terms of the 2HDM is discussed in Section III. Section IV focuses on the direct CP-measurement of the heavy scalar resonance through spin correlations. Finally, a summary of our key findings is delivered in Section V.

II. ANALYSIS

We study the signature of a pseudoscalar $J^\pi = 0^-$ state produced in association with a top pair $t\bar{t}A$ at the 13 TeV LHC. We access this channel via the decay $A \rightarrow b\bar{b}$ along with di-leptonic tops. To simulate the signal, we resort to a Simplified Model which describes the dynamics of the 0^- state through the interaction Lagrangian

$$\mathcal{L} \supset \kappa_t \frac{iy_t A \bar{t} \gamma_5 t}{\sqrt{2}} + \kappa_b \frac{iy_b A \bar{b} \gamma_5 b}{\sqrt{2}}, \quad (1)$$

where $y_{t(b)} \equiv \sqrt{2}m_{t(b)}/v$ are the SM Yukawa couplings to top (bottom) quarks, with the Higgs vev $\langle H \rangle = v/\sqrt{2} \simeq 246$ GeV. This is a four-parameter model, where the input quantities are chosen to be: the pseudoscalar mass m_A , its width Γ_A , and the top (bottom) rescaling factors $\kappa_{t(b)}$, through which we can test the relative strength of their respective Yukawas to the new 0^- resonance. By keeping Γ_A as a free parameter, we allow our framework to accommodate additional pseudoscalar couplings to other new degrees of freedom. As we will discuss in more detail in Section III, such a generic Simplified Model setup dovetails with a broad class of more specific new physics models such as extended Higgs sectors like the 2HDM, or Dark Matter (DM) models [18–22]. For the latter, the Lagrangian in Eq. 1 can be extended with the extra pseudoscalar mediator coupled also to the DM particle. This way, the strategy we explore in this paper can be seen as the counterpart of a DM search where, instead of probing the mediator decays to the Dark Sector, we now test the interactions of the pseudoscalar bouncing back to the SM.

To control the backgrounds, we require four b-tagged jets. The major backgrounds are $t\bar{t}b\bar{b}$ and

$t\bar{t}Z$. The $t\bar{t}A$ signal sample is generated with MADGRAPH5+PYTHIA8 [23, 24], while for the backgrounds $t\bar{t}b\bar{b}$ and $t\bar{t}Z$ we use SHERPA+OPENLOOPS [25, 26]. A proper modelling for the QCD effects is of major importance in this study as the Higgs is part of a multi-jet system. Hence, we simulate all samples at Next-to-Leading Order (NLO) QCD with the MC@NLO algorithm [27]. To evaluate the signal decay rates $A \rightarrow b\bar{b}$, we use the 2HDM predictions from the HDECAY [28] package, with appropriately rescaled Yukawas via the parameter $\tan\beta$ (cf. Section III further down). Additional non-SM effects from higher orders are precluded by setting the *alignment limit* condition $\cos(\beta - \alpha) = 0$. Spin correlation effects in the top decays are fully accounted for in our simulation [29, 30]. We also consider the hadronisation and underlying event effects with the PYTHIA8 and SHERPA modules.

We start our analysis by requiring two isolated opposite sign leptons with $p_{T\ell} > 15$ GeV and $|\eta_\ell| < 2.5$. The leptons are defined as isolated if there is less than 20% of hadronic activity around the leptonic radius $R = 0.2$. For the hadronic part of the event, we start by reclustering jets with the Cambridge/Aachen (C/A) jet-algorithm with the FASTJET package [31].

The opening angle between the two b -quarks generated from the pseudoscalar decay can be estimated in the boosted regime by

$$\Delta R_{b\bar{b}} \sim \frac{2m_A}{p_{TA}}, \quad (2)$$

where p_{TA} stands for the pseudoscalar transverse momentum. As we probe a wide range of pseudoscalar masses, we customise our search with different jet radius R for distinct pseudoscalar mass range hypotheses: $R = 0.6, 1.2$ and 2.4 for $m_A = [20, 100)$, $[100, 200]$ GeV and $(200, 400]$ GeV, respectively. We require at least one fat jet with $p_{TJ} > 200$ GeV and $|\eta_J| < 2.5$. This transverse momentum selection on the fat-jet is enhanced to $p_{TJ} > 310$ GeV for very large pseudoscalar masses $m_A = (300, 400]$ GeV. Instead of requiring a larger jet radius $R > 2.4$, which would also collect undesired radiation from the top decays, we find more efficient to demand a larger transverse momentum selection in this regime.

The fat-jet is demanded to be tagged by the BDRS algorithm [15]. The BDRS *filtering* promotes the invariant fat-jet mass to be a robust observable as it efficiently controls the pile-up effects [32]. The two hardest sub-jets from this tagged jet are then b -tagged. We adopt 70% b -tagging efficiency and 1% misstag rate [33].

For the remaining hadronic activity, we remove the tagged fat-jet and recluster jets again with C/A but now with $R = 0.5$, $p_{Tj} > 30$ GeV and $|\eta_j| < 2.5$. The smaller jet radius suppresses the possible underlying event contamination. We require two extra b-tagged jets to suppress the possible extra backgrounds. Lastly, we demand the filtered fat-jet mass m_A^{BDRS}

	C/A $R = 0.6$			C/A $R = 1.2$			C/A $R = 2.4$		
	ttA_{50}	$t\bar{t}b\bar{b}$	$t\bar{t}Z$	ttA_{150}	$t\bar{t}b\bar{b}$	$t\bar{t}Z$	ttA_{200}	$t\bar{t}b\bar{b}$	$t\bar{t}Z$
BDRS A -tag, $p_{T\ell} > 15$ GeV, $ \eta_\ell < 2.5$	1.08	7.95	0.99	0.63	10.93	1.11	0.52	11.69	1.29
$n_\ell = 2$, $p_{Tj} > 30$ GeV, $ \eta_j < 2.5$, $n_j \geq 2$	0.43	3.77	0.19	0.26	4.21	0.21	0.14	3.11	0.14
two extra b-tags – four in total	0.22	0.35	–	0.085	0.26	–	0.05	0.35	–
$ m_A^{BDRS} - m_A /m_A < 0.15$	0.15	0.10	–	0.06	0.21	–	0.04	0.20	–
$m_{ii} > 75$ GeV									

Table I. Signal and background cut-flow analysis for the LHC at $\sqrt{s} = 13$ TeV. Rates are shown in fb accounting for b-tagging efficiencies, hadronisation and underlying event effects. For illustrative purposes, we display the results for three different signal hypotheses $m_A = 50, 150, 200$ GeV calculated respectively with $C/A R = 0.6, 1.2, 2.4$. The branching ratios $\mathcal{BR}(A \rightarrow b\bar{b})$ are calculated with HDECAY is included and we assume $\tan\beta = 1$. All signal and backgrounds samples are produced at NLO precision with the MC@NLO algorithm.

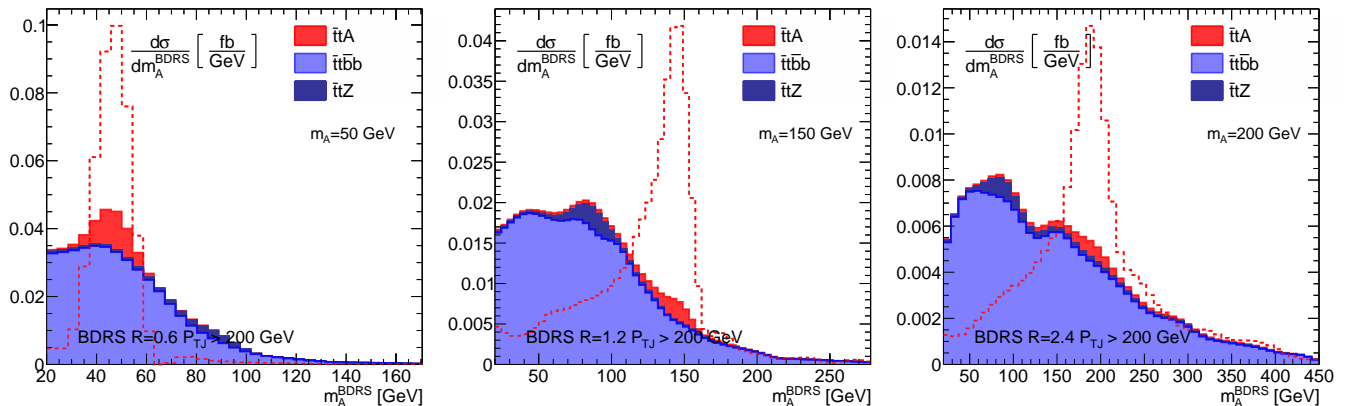


Figure 1. Signal and background invariant mass distribution for the BDRS tagged fat-jet m_A^{BDRS} . We show the three different signal hypotheses presented on Tab. I: $m_A = 50, 150, 200$ GeV calculated respectively with $C/A R = 0.6, 1.2, 2.4$. The histograms are stacked. We also display the normalised signal component to the total background rate (red dashed).

to be in a window centered on the pseudoscalar mass m_A , $|m_A^{BDRS} - m_A|/m_A < 0.15$. The cut-flow analysis is displayed in Tab. I. For illustrative purposes, we show the results for three different signal hypotheses $m_A = 50, 150, 200$ GeV with $\tan\beta = 1$.

The signal and backgrounds invariant mass distributions m_A^{BDRS} are shown in Fig. 1. We display the three different signal hypotheses presented on Tab. I. The results include event selections up to the four b-jet tagging. The signal displays a clear peak structure around the resonance mass, m_A , for all considered cases. We emphasise that this was only achievable after tailoring the jet substructure analysis in different mass regions through convenient fat-jet radius R and transverse momentum selection p_{Tj} , as previously described.

Within our Simplified Model framework, the signal cross section – or more generally any signal distribution – can be written as $\sigma_{sig} = \kappa_t^2 \kappa_b^2 \sigma(m_A, \Gamma_A)$. Therefore, the analysis depends only on three parameters: the pseudoscalar mass m_A , its width Γ_A , and the product of the rescaling couplings to tops and bottoms $\kappa_t \kappa_b$. These parameters are only bound *a priori* to the consistency condition

$$\Gamma_A \geq \Gamma_{A \rightarrow t\bar{t}} + \Gamma_{A \rightarrow b\bar{b}}, \quad (3)$$

which reflects that the pseudoscalar state is likely part of a larger UV completion, with possibly additional decay modes besides the explicit ones in our Simplified Model. For simplicity, we fix $\Gamma_A = 0.05m_A$ throughout our Simplified Model analysis.

Based on the presented collider study, we can derive constraints on the Simplified Model parameters by further exploring the kinematics of the leptonic top decays via a two-dimensional binned log-likelihood analysis on $(\Delta\eta_\ell, \Delta\phi_\ell)$. See Sec. IV for a detailed discussion on the $\Delta\phi_\ell$ sensitivity. In Fig. 2 we display the 95% CL limits on $\sqrt{\kappa_t \kappa_b}$ as a function of the pseudoscalar mass m_A . The accessible regions are limited from above and below. The upper bound originates from the consistency condition Eq. (3). For all points inside the red area, the partial pseudoscalar widths to tops and bottoms would surpass the assumed total width, $\Gamma_A = 0.05m_A$. The lower bound stems from the limited statistics, as for all points below the light (dark) blue bands would yield unobservable signal rates at the 13 TeV LHC after 300 (3000) fb^{-1} of integrated luminosity.

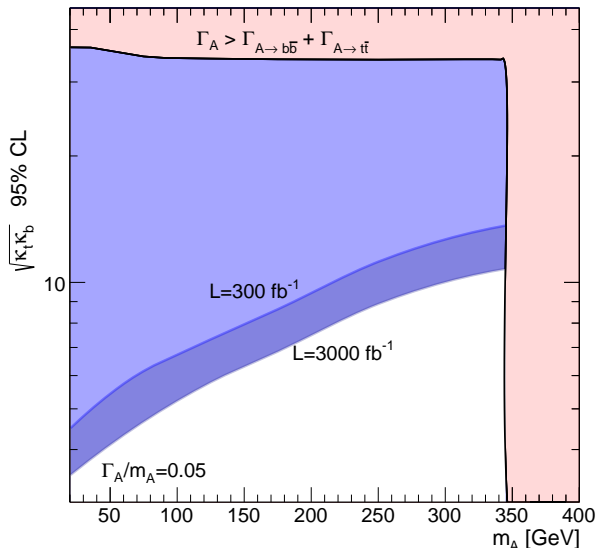


Figure 2. 95% CL exclusion region on $\sqrt{\kappa_t \kappa_b}$ as a function of the pseudoscalar mass m_A in the Simplified Model framework Eq. 1. The shaded regions in blue can be excluded by the 13 TeV LHC with $\mathcal{L} = 300 \text{ fb}^{-1}$ (light blue) and 3000 fb^{-1} (dark blue). The shaded region in red cannot be probed and is given by the consistency constraint $\Gamma_A \geq \Gamma_{A \rightarrow t\bar{t}} + \Gamma_{A \rightarrow b\bar{b}}$. We assume $\Gamma_A/m_A = 0.05$.

III. A BSM SCENARIO

A. Extended Higgs sector

Thus far we have applied our $t\bar{t}A(b\bar{b})$ analysis to the test-ground Simplified Model laid out by the Lagrangian (1). By trading completeness in favor of generality and a minimal number of new parameters and fields, Simplified Models of this guise have become a cherished toolkit to analyse plausible new physics signal topologies and to interpret the results of collider searches [34]. In the following, we promote our search strategy to a more realistic extended Higgs sector. Our prime candidate is the 2HDM [35, 36]. In addition to its indisputable interest for Higgs coupling analyses [37–39], collider searches [40], and beyond the SM phenomenology [41], the 2HDM describes the low-energy Higgs sector of a variety of TeV-scale new physics models [42], and contains all the necessary ingredients to reinterpret the above Simplified Model analysis:

1. A CP-odd scalar A , which is present in the 2HDM physical spectrum, along with two neutral CP-even scalars h, H and a pair of charged scalars H^\pm ;
2. A limit of *alignment without decoupling* [43, 44], in which one of the neutral CP-even mass eigenstates mimics the SM Higgs boson, while at least one of the extra resonances remains relatively light. Precisely due to the excellent agreement with the LHC data, the *alignment limit* is strongly favored by the global LHC fits [45] - and at the same time very

	h	H	A
κ_t	$\frac{\cos \alpha}{\sin \beta}$	$\frac{\sin \alpha}{\sin \beta}$	$\cot \beta$
κ_b	$-\frac{\sin(\alpha - \gamma_b)}{\cos(\beta - \gamma_b)}$	$\frac{\cos(\alpha - \gamma_b)}{\cos(\beta - \gamma_b)}$	$\tan(\beta - \gamma_b)$

Table II. Neutral Higgs boson couplings to fermions in a generic 2HDM, where the Yukawa interactions follow a flavor alignment pattern parametrised through the independent angle γ_b in the notation of [50].

difficult to probe, unless the additional states are not decoupled, and hence possible to pin down at colliders. This is therefore the natural scenario our strategy suits best.

3. A minimal, UV complete embedding for fully flexible couplings [46], which in particular allow for both enhanced and suppressed fermion Yukawas. This is possible in the 2HDM as it includes two weak doublets which can couple to fermions and gauge bosons independently, unlike other models such as the singlet extension [47].

At variance with the couplings to the weak bosons, the Higgs-fermion Yukawas are not uniquely determined by the underlying gauge structure. The four canonical 2HDM setups [36] are obtained by imposing a global \mathcal{Z}_2 invariance $\Phi_{1,2} \rightarrow \mp \Phi_{1,2}$ and linking each fermion family to only one of the Higgs doublets Φ_i . In turn, these are particular cases of the more general *Minimal Flavor Violation* category [48], which include among others the so-called *flavor-aligned* 2HDM [49]. The Yukawa structures in the latter case can be parametrised through independently variable angles (cf. Tab. II) and may be seen as an interpolation between the canonical Type-I ($\gamma_b = \pi/2$) and Type-II models ($\gamma_b = 0$).

For a given choice of γ_b , our $t\bar{t}A(b\bar{b})$ -based strategy directly tests the 2-dimensional slice $(m_A, \tan \beta)$. The parameter $\tan \beta$ denotes as customary the *vev* ratio $\tan \beta \equiv \langle \Phi_2 \rangle / \langle \Phi_1 \rangle = v_2/v_1$ of the individual Higgs fields. In the *alignment limit*, the second mixing angle α , which parametrises the rotation of the neutral CP-even gauge-eigenstates into the physical fields h, H , is fixed through either $\cos(\beta - \alpha) = 0$ or $\sin(\beta - \alpha) = 0$. Mapping these parameters back onto the Simplified Model Lagrangian (1), we find

$$\kappa_t = \cot \beta; \quad \kappa_b = \tan(\beta - \gamma_b) = \frac{\tan \beta - \tan \gamma_b}{1 + \tan \beta \tan \gamma_b}. \quad (4)$$

Accordingly, the exclusion contours for $\sqrt{\kappa_t \kappa_b}$ in Fig. 2 impose constraints on $\tan \beta$ for every given γ_b and pseudoscalar mass hypothesis m_A . Eq. (4) makes it patent that the sensitivity attainable by the $t\bar{t}A(b\bar{b})$ analysis becomes optimal for a Type-I setup and slight variations thereof ($\gamma_b \simeq \frac{\pi}{2}$), where both the top and the bottom Yukawas increase simultaneously for $\tan \beta < 1$ as

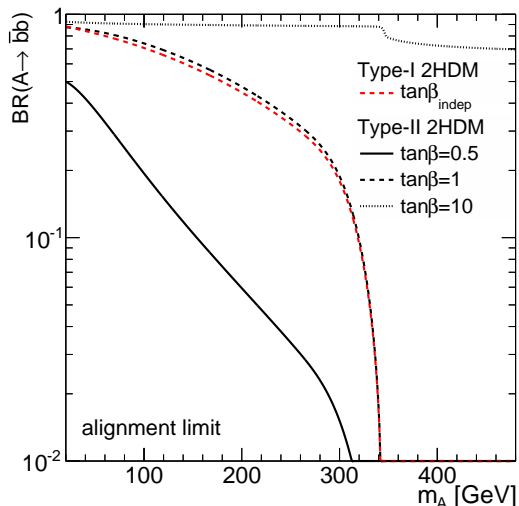


Figure 3. Branching ratio $\mathcal{BR}(A \rightarrow \bar{b}b)$ as a function of the pseudoscalar mass m_A for Type-I (red) and Type-II (black) 2HDM for exemplary scenarios in the *alignment limit*.

$\sqrt{\kappa_t \kappa_b} = 1/\tan\beta$, generating a quadratic signal strength dependence $\mu_{\text{sig}} \propto \cot^2\beta$. In contrast, this search is loosely efficient for Type-II, where the top and the bottom Yukawas have inverse scalings with respect to each other. Here, a growth in the $\bar{t}tA$ production rate is counterbalanced by a suppressed $A \rightarrow \bar{b}b$ decay. The dependence on $\tan\beta$ is marginal here, and features merely through the total decay width Γ_A .

To better visualize the key parameter dependences, in Fig. 3 we display the pseudoscalar branching ratio $\mathcal{BR}(A \rightarrow \bar{b}b)$ as a function of its mass m_A . All decay rates are computed with HDECAY [28] for the 2HDM in the *alignment limit*. For definiteness we assume no additional chain decays $A \rightarrow hZ, HZ, H^\pm W^\pm$. For the Type-II model we choose as illustrative *vev* ratios $\tan\beta = 0.1, 1, 30$, while for Type-I the results do not depend on $\tan\beta$. We see how $\mathcal{BR}(A \rightarrow \bar{b}b)$ is enhanced (suppressed) for large (small) values of $\tan\beta$ in the Type-II 2HDM, reflecting the different rescalings of the top and the bottom Yukawas. The steep fall around $m_A \gtrsim 2m_t$ signals the opening of the top pair mode $A \rightarrow \bar{t}t$. In a Type-II model with sufficiently large $\tan\beta$, the enhanced bottom Yukawa explains why $A \rightarrow \bar{b}b$ dominates even above the top pair threshold. The mild, yet visible, offset between the $\mathcal{BR}(A \rightarrow \bar{b}b)$ curves for the Type-I with respect to the Type-II 2HDM at $\tan\beta \simeq 1$ follows from the different relative signs between the top and the bottom Yukawas, which feature through the top and bottom loop interferences contributing to the loop-induced modes $A \rightarrow gg, \gamma\gamma$.

BI: $m_A > 125$ $\cos(\beta - \alpha) = 0$	
• $m_h = 125$	• $m_H = (220 - 300)$
• $m_{H^\pm} = \max(175, m_A)$	• $m_{12}^2 = \frac{m_A^2 \tan\beta}{1 + \tan^2\beta}$
BII: $63 < m_A < 125$ $\sin(\beta - \alpha) = 0$	
• $m_h = 120$	• $m_H = 125$
• $m_{H^\pm} = 175$	• $m_{12}^2 = 0$
BIII: $m_A < 63$ $\sin(\beta - \alpha) = 0$	
• $m_h = 120$	• $m_H = 125$
• $m_{H^\pm} = 175$	• $m_{12}^2 = \frac{(m_H^2 + 2m_A^2) \tan\beta}{2(1 + \tan^2\beta)}$

Table III. Sample benchmarks for a Type-I 2HDM in the different patches of the $m_A - \tan\beta$ plane covered by the $\bar{t}tA(\bar{b}b)$ search. All masses are given in GeV.

B. Parameter space

In the following, we illustrate how our proposed search strategy is capable to constrain phenomenologically viable 2HDM scenarios in the well-motivated *alignment without decoupling* limit. For that, in Tab. III, we identify exemplary benchmarks spanning the $m_A - \tan\beta$ plane tested by our search. For definiteness, we stick hereafter to quark Yukawa couplings of Type-I.

We separately cover the two relevant pseudoscalar mass ranges, namely above (below) the SM Higgs mass. For $m_A > 125$ GeV (resp. $m_A < 125$ GeV) we assume a *direct* (flipped) CP-even eigenmass ordering, fixing the SM-like Higgs mass to $m_h = 125$ GeV ($m_H = 125$ GeV) and $\beta - \alpha$ through the appropriate *alignment* condition. The bosonic chain decays $A \rightarrow hZ, HZ, H^\pm W^\pm$ do not contribute in any case. Compatibility with all model constraints we assess through an in-house interface of the public tools 2HDMC [51], HIGGSBOUNDS [52], SUPERISO [53] and HIGGSSIGNALS [54] along with additional own routines (cf. also [55] for an up-to-date review). The average LHC signal strength of the SM Higgs boson is by construction satisfied in the *alignment limit*, with the proviso that non-standard Higgs decays are suppressed or simply closed. For that, in the BIII region we fix the Z_2 soft-breaking mass m_{12}^2 [36] such that the mode $H \rightarrow AA$ vanishes at tree-level. The relatively small mass splittings between the different additional Higgs states agree with Electroweak Precision Observables [56, 57]. The lines $m_{12}^2 \simeq m_A^2 \tan\beta / (1 + \tan^2\beta)$ and $m_{12}^2 = 0$ for the BI (resp. BII) regions satisfy unitarity [58, 59], perturbativity [60] and vacuum stability [61]. We test values of $\tan\beta$ down to ~ 0.1 , assuming that these already border the onset of a strongly-coupled regime.

The key feature of the *alignment without decoupling* scenarios, such as those in Tab. III, is that the additional Higgs states remain light or only moderately heavy. This means that the chief constraints on them are imposed by the direct LEP, Tevatron, and LHC searches. The condition $m_{H^\pm} \gtrsim 175$ GeV follows from the limits on

charged scalars [62], which hinder the non-standard top decay $t \rightarrow H^\pm b \rightarrow \tau \nu_\tau b$. Depending on the underlying assumptions, certain parameter space patches in Tab. III with enhanced fermion Yukawas would be strongly disfavored by the CP-even [63–65] and CP-odd searches [63–68, 74, 75]. If the 2HDM was to be strictly taken as an UV completion, it would first of all be difficult to reconcile $\tan\beta < 1$ with the $pp \rightarrow H, A \rightarrow \gamma\gamma$ searches in the $m_{H,A} < 300$ GeV range. A more flexible approach, which we follow here, is to consider the 2HDM as part of a larger UV completion, where additional charged states compensate the enhanced top loops in $H, A \rightarrow \gamma\gamma$. The same argument can be advocated to evade the indirect constraints for $\tan\beta \lesssim 1$ from charged Higgs loops in $B_d - \bar{B}_d$ and $B_s^0 \rightarrow \mu^+\mu^-$ [76]. Also important is the role of di-tau final-states [64, 65]. In a strict Type-I interpretation, these would rule out a sizeable portion of the range $\tan\beta < 1$, $m_A \gtrsim 105$ GeV covered by Tab. III. Such constraints can be eluded by assuming in this case lepton-specific (viz. Type-II) couplings, while keeping a Type-I setup for the quarks. Yet, some of the patches with $\tan\beta \simeq 1$ and $m_A \simeq (110 - 180)$ GeV remain in tension with the recent LHC results [66]. Likewise, $\tan\beta \lesssim 0.6$ is precluded for $m_{H,A} \lesssim 120$ GeV by the Tevatron analysis $p\bar{p} \rightarrow \tau\bar{\tau}H \rightarrow \tau\bar{\tau}\tau\bar{\tau}$ [75]. Finally, the lowest m_A edge are in conflict with the LHC search $pp \rightarrow t\bar{t}(H, A) \rightarrow t\bar{t}t\bar{t}$ [67] and also ruled out in part by the LEP search $e^+e^- \rightarrow hA \rightarrow b\bar{b}b\bar{b}$ [68].

The benchmark regions in Tab. III serve us to promote our $t\bar{t}A(b\bar{b})$ search strategy beyond a mere Sim-

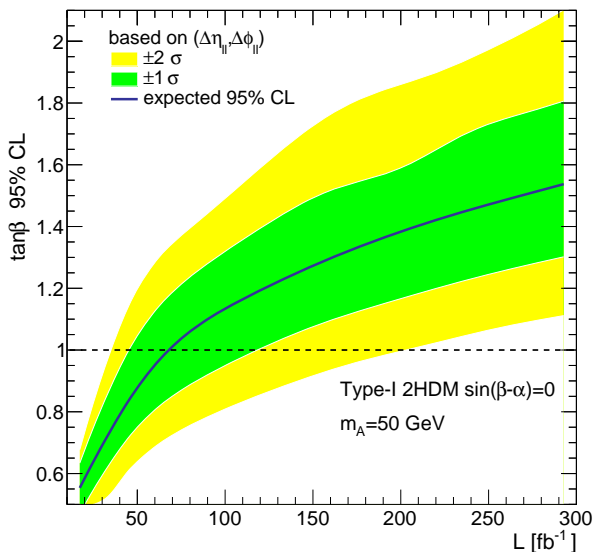


Figure 4. 95% CL bound on $\tan\beta$ as a function of the LHC luminosity from the $t\bar{t}A(b\bar{b})$ search. The binned log-likelihood analysis is based on the two-dimensional distribution $(\Delta\eta_u, \Delta\phi_u)$. We illustrate our results taking as exemplary case a Type-I 2HDM with $m_A = 50$ GeV.

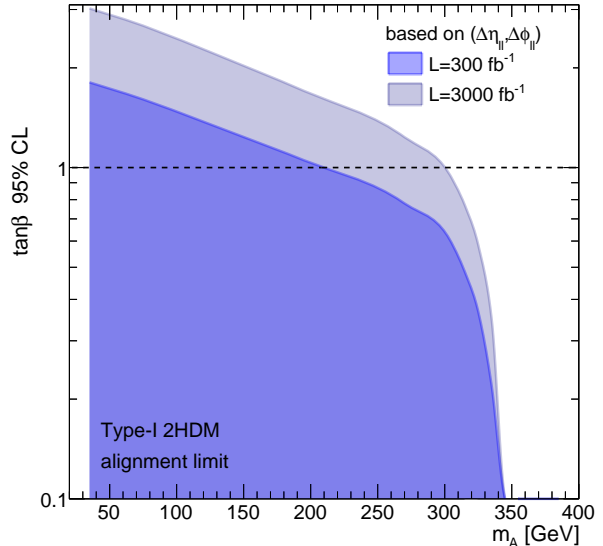


Figure 5. 95% CL exclusion region on $\tan\beta$ as a function of the pseudoscalar mass m_A for Type-I 2HDM with fixed LHC integrated luminosity: $\mathcal{L} = 300 \text{ fb}^{-1}$ (blue) and $\mathcal{L} = 3000 \text{ fb}^{-1}$ (gray).

plified Model framework, assessing its implications for a phenomenologically viable, UV complete, extended Higgs sector. This exercise we perform in Fig. 4. Here we remap the Simplified Model constraints of Fig. 2 onto the Type-I 2HDM in the *alignment limit*. The 95% CL bound follows from the two-dimensional binned log-likelihood analysis of the $t\bar{t}A$ kinematics in the variables $(\Delta\eta_u, \Delta\phi_u)$, as explained earlier on. The limits on $\tan\beta$ are obtained as a function of the LHC integrated luminosity, for a fixed pseudoscalar mass hypothesis $m_A = 50$ GeV. We find that, over the Run II, the LHC would be capable to bound the range $\tan\beta > 1$ with only 70 fb^{-1} , and climb up to $\tan\beta > 1.5$ with 300 fb^{-1} of collected data. For $\tan\beta$ above these values, the number of signal events would not be observable. Such a remarkable sensitivity on $\tan\beta$ we can ultimately trace back to the characteristic signal strength dependence $\mu_{\text{sig}} \propto \cot^2\beta$ in the Type-I 2HDM, resulting from the $\cot\beta$ -rescaled top Yukawa along with the $\tan\beta$ -independent $\mathcal{BR}(A \rightarrow b\bar{b})$.

Additionally, in Fig. 5 we display the 95% CL bound for the same Type-I 2HDM setup, now as a function of the m_A . The proposed $t\bar{t}A(b\bar{b})$ analysis can set a limit $\tan\beta > 1$ for $20 \text{ GeV} < m_A < 210 \text{ GeV}$ with $\mathcal{L} = 300 \text{ fb}^{-1}$ and probe masses up to $m_A \sim 320$ GeV at the high luminosity LHC $\mathcal{L} = 3000 \text{ fb}^{-1}$, achieving a remarkable sensitivity up to $m_A \sim 2m_t$. Obviously, above the top pair production threshold, the $A \rightarrow t\bar{t}$ decay holds the largest constraining power [8].

IV. CP MEASUREMENT: $t\bar{t}A$ VS. $t\bar{t}H$

In the *alignment limit*, the Yukawa patterns of both the heavy CP-even (H) and the CP-odd (A) 2HDM resonances follow, up to sign differences, an identical dependence on $\tan\beta$, see Tab. IV. This means that both CP

	Type-I		Type-II	
	H	A	H	A
κ_t	$-\cot\beta$	$\cot\beta$	$-\cot\beta$	$\cot\beta$
κ_b	$-\cot\beta$	$-\cot\beta$	$\tan\beta$	$\tan\beta$

Table IV. Relative coupling strength $\kappa_{t(b)}$ for top (bottom) quarks with respect to the SM Yukawa couplings for the Type-I and Type-II 2HDM scenarios in the alignment limit.

hypotheses would exhibit very similar signatures when searching for heavy 2HDM resonances in the *alignment limit* through fermionic channels. In the event of a signal excess, an immediate question would hence be to characterise the CP properties of the discovered heavy state. In this section, we demonstrate how a direct CP measurement of a heavy 2HDM candidate is possible by examining the spin correlations in fermionic final states [17, 69–72]. As CP-sensitive quantity, we follow Ref. [17] and choose the angular correlation variable $\Delta\phi_{ll}$: that is, the difference in azimuthal angle around the beam axis of the top-pair leptonic decay products in the lab-frame. This strategy, originally applied to the 125 GeV Higgs in Ref. [17], benefits from the more boosted $A(H)$ kinematics we must require for the signal to be observable. The increased CP-sensitivity in the boosted regime is ultimately correlated to the enhancement of the mixed helicity states $t_L\bar{t}_R + t_R\bar{t}_L$ in the large $p_{T,A(H)}$ region. Interestingly, this helicity state presents different modulations in the azimuthal top pair angle $\Delta\phi_{tt}$, which manifest as oscillations obeying $\sin\Delta\phi_{tt}$ (resp. $\cos\Delta\phi_{tt}$) when the top pair is produced in association with a CP-even (resp. CP-odd) scalar. The analytic argument is elaborated in detail in Ref. [17].

In Fig. 6 we compare the lab-frame $\Delta\phi_{ll}$ distributions for the CP-odd ($t\bar{t}A$) and the CP-even ($t\bar{t}H$) signal hypotheses, together with the $t\bar{t}b\bar{b}$ background after the selection cuts given in Tab. I. The latter we supplement now with an additional cut on the di-lepton invariant mass $m_{ll} > 75$ GeV. This extra requirement works as a proxy for the di-leptonic top pair selection m_{tt} [73], further enhancing the unlike-helicity states. To generate the signal events, we assume a Type-I 2HDM and for definiteness fix $\tan\beta = 0.5$ and $m_{A(H)} = 150$ GeV. As we can see, the analysis of the $\Delta\phi_{ll}$ distributions provides an efficient procedure to discriminate between the two competing hypotheses. Notably, the sensitivity reaches up to $\sigma_{t\bar{t}A}/\sigma_{t\bar{t}H} \sim 2$ for small angles $\Delta\phi_{ll} \sim 0$.

Besides its remarkable CP-sensitivity, the chosen variable $\Delta\phi_{ll}$ is also advantageous from the experimental viewpoint. Thanks to the fact that it exclusively relies on the leptons, and that it is reconstructed in the lab-frame,

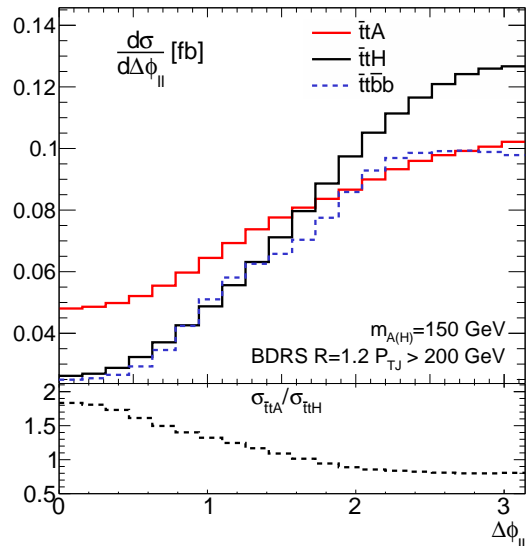


Figure 6. Azimuthal angular distribution $\Delta\phi_{ll}$ between the two leptons for the CP-odd $t\bar{t}A$ (red) and CP-even $t\bar{t}H$ (black) signal hypotheses and $t\bar{t}b\bar{b}$ (blue) background. We assume a Type-I 2HDM with $\tan\beta = 0.5$ and $m_{A(H)} = 150$ GeV.

it is affected by rather small experimental uncertainties. In particular, it does not suffer from the usual uncertainties associated e.g. to the top reconstruction or a reference frame change.

It also worth noticing that by including the $\Delta\phi_{ll}$ distribution in the previous $t\bar{t}A(b\bar{b})$ analysis, namely in the binned log-likelihood test of Figs. 2, 4 and 5, we achieve

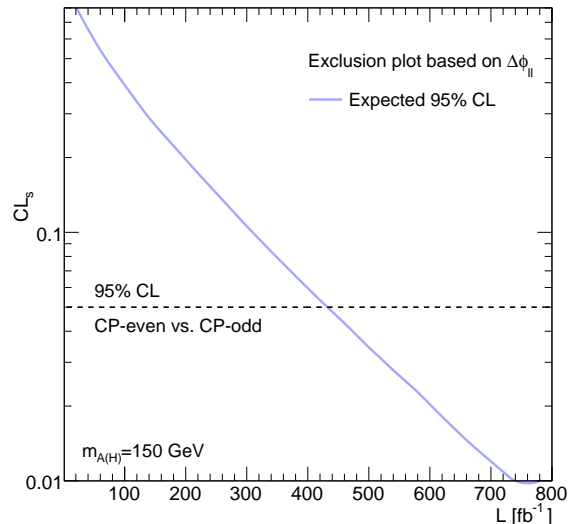


Figure 7. Luminosity needed to distinguish the CP-odd $t\bar{t}A$ from the CP-even $t\bar{t}H$ signal hypotheses at 95% CL. We assume a Type-I 2HDM with $\tan\beta = 0.5$ and $m_{A(H)} = 150$ GeV.

a significantly improved signal over background (\mathcal{S}/\mathcal{B}) separation. This reflects the different angular modulations for the $t\bar{t}A$ signal and $t\bar{t}b\bar{b}$ background that, for our showcase signal scenario in Fig. 6, result in enhanced sensitivities $\sigma_{t\bar{t}A}/\sigma_{t\bar{t}b\bar{b}} \sim 2$ for small angles $\Delta\phi_{ll} \sim 0$.

Finally, in Fig. 7 we quantify the statistical power of our proposed CP discriminant, by performing a binned log-likelihood test based on the $\Delta\phi_{ll}$ distribution. To focus exclusively on the power of the spin correlation measurement, we set both $t\bar{t}A$ and $t\bar{t}H$ event rates to the same value $\sigma_{t\bar{t}A}$, which we compute for our trial setup of a Type-I 2HDM with $\tan\beta = 0.5$ and $m_{A(H)} = 150$ GeV. In this plot we show the luminosity needed to directly distinguish the two alternative CP hypotheses at 95% CL in the 13 TeV LHC run. We observe that this can be achieved after collecting ~ 450 fb^{-1} of data, for the assumed number of signal events. Let us emphasise that this result should be interpreted only as an upper bound. A more accurate estimate would for instance be possible by including the three b -tag sample, mostly if in conjunction with possible improvements on the misstag rate [77], or accounting for additional observables combined within a Boosted Decision Tree [78].

V. SUMMARY

In this letter, we have focused on the quest for signatures of an additional pseudoscalar boson at the LHC. We have concentrated on moderate pseudoscalar masses and scrutinised a range of variable couplings to the top and bottom quarks, which we describe in a Simplified Model setup, where the novel resonance interacts with the heavy quarks through independently rescaled Yukawa couplings. To test these interactions, we devise a search strategy based on the associated pseudoscalar production along with a $t\bar{t}$ pair, followed by the decay $A \rightarrow b\bar{b}$ and

with di-leptonic top signatures. By using jet substructure techniques, conveniently tailored to different pseudoscalar mass ranges, we are able to provide an ample coverage of the possible new resonance masses. First, we apply our collider analysis to obtain limits on the parameter space of the Simplified Model. We then reinterpret these results in light of a 2HDM in the *alignment without decoupling* limit. In particular we show that, for a Type-I 2HDM pattern of heavy quark Yukawas, and after collecting 300 fb^{-1} of data, it would be possible to *i)* constrain the region $\tan\beta > 1.5$ at 95 % CL for a light pseudoscalar of $m_A = 50$ GeV; and *ii)* exclude the entire mass range $20 \text{ GeV} < m_A < 210 \text{ GeV}$ with $\tan\beta \leq 1$. Finally, we analyse the spin correlations of the final-state fermions. We show that the difference in azimuthal angle between the leptons from the top decays $\Delta\phi_{ll}$ in the lab-frame critically depends on the CP nature of the heavy 2HDM scalar, providing a direct handle on the quantum numbers of the resonance candidate.

In view of its paramount implications for the particle physics puzzle, unveiling footprints of additional scalars ranks very high in the wish-list of new physics chasers. As we have demonstrated, collider searches based on heavy-quark-rich final states are called to play a decisive role in this task - now that the unleashed discovery power of the LHC at Run II starts crossing the borders of the multi-TeV territory.

Acknowledgments

DLV is funded by the F.R.S.-FNRS *Fonds de la Recherche Scientifique* (Belgium). DG is thankful to the Mainz Institute for Theoretical Physics (MITP) for its hospitality and partial support during the completion of this work.

-
- [1] G. Aad *et al.* [ATLAS Collaboration], Phys. Lett. B **716**, 1 (2012); S. Chatrchyan *et al.* [CMS Collaboration], Phys. Lett. B **716**, 30 (2012).
- [2] P. W. Higgs, Phys. Rev. Lett. **13**, 508 (1964); P. W. Higgs, Phys. Lett. **12**, 132 (1964). doi:10.1016/0031-9163(64)91136-9
- [3] F. Englert and R. Brout, Phys. Rev. Lett. **13**, 321 (1964).
- [4] G. S. Guralnik, C. R. Hagen and T. W. B. Kibble, Phys. Rev. Lett. **13**, 585 (1964).
- [5] T. Corbett, O. J. P. Eboli, D. Goncalves, J. Gonzalez-Fraile, T. Plehn and M. Rauch, JHEP **1508**, 156 (2015).
- [6] V. Khachatryan *et al.* [CMS Collaboration], JHEP **1511**, 071 (2015).
- [7] CMS Collaboration [CMS Collaboration], CMS-PAS-HIG-14-030.
- [8] N. Craig, F. D'Eramo, P. Draper, S. Thomas and H. Zhang, JHEP **1506**, 137 (2015).
- [9] S. Gori, I. W. Kim, N. R. Shah and K. M. Zurek, Phys. Rev. D **93**, no. 7, 075038 (2016).
- [10] J. Hajer, Y. Y. Li, T. Liu and J. F. H. Shiu, JHEP **1511**, 124 (2015).
- [11] N. Craig, J. Hajer, Y. Y. Li, T. Liu and H. Zhang, arXiv:1605.08744 [hep-ph].
- [12] J. Kozaczuk and T. A. W. Martin, JHEP **1504**, 046 (2015).
- [13] M. Casolino, T. Farooque, A. Juste, T. Liu and M. Spannowsky, Eur. Phys. J. C **75**, 498 (2015) doi:10.1140/epjc/s10052-015-3708-y [arXiv:1507.07004 [hep-ph]].
- [14] W. Buchmuller and D. Wyler, Nucl. Phys. B **268**, 621 (1986). B. Grzadkowski, M. Iskrzynski, M. Misiak and J. Rosiek, JHEP **1010**, 085 (2010).
- [15] J. M. Butterworth, A. R. Davison, M. Rubin and G. P. Salam, Phys. Rev. Lett. **100**, 242001 (2008).
- [16] T. Plehn, G. P. Salam and M. Spannowsky, Phys. Rev. Lett. **104**, 111801 (2010).

- [17] M. R. Buckley and D. Goncalves, Phys. Rev. Lett. **116**, no. 9, 091801 (2016).
- [18] M. R. Buckley, D. Feld and D. Goncalves, Phys. Rev. D **91**, 015017 (2015).
- [19] D. Goncalves, F. Krauss, S. Kuttimalai and P. Maierhofer, arXiv:1605.08039 [hep-ph].
- [20] P. Harris, V. V. Khoze, M. Spannowsky and C. Williams, Phys. Rev. D **91**, 055009 (2015) doi:10.1103/PhysRevD.91.055009 [arXiv:1411.0535 [hep-ph]].
- [21] U. Haisch, F. Kahlhoefer and J. Unwin, JHEP **1307**, 125 (2013) doi:10.1007/JHEP07(2013)125 [arXiv:1208.4605 [hep-ph]].
- [22] J. Abdallah *et al.*, Phys. Dark Univ. **9-10**, 8 (2015) doi:10.1016/j.dark.2015.08.001 [arXiv:1506.03116 [hep-ph]].
- [23] J. Alwall, M. Herquet, F. Maltoni, O. Mattelaer and T. Stelzer, JHEP **1106**, 128 (2011).
- [24] T. Sjostrand, S. Mrenna and P. Z. Skands, Comput. Phys. Commun. **178**, 852 (2008).
- [25] T. Gleisberg, S. Höche, F. Krauss, M. Schönherr, S. Schumann, F. Siegert and J. Winter, JHEP **0902**, 007 (2009); F. Krauss, R. Kuhn and G. Soff, “AMEGIC++ 1.0: A Matrix element generator in C++,” JHEP **0202**, 044 (2002); T. Gleisberg and S. Hoeche, JHEP **0812** (2008) 039. T. Gleisberg and F. Krauss, Eur. Phys. J. C **53** (2008) 501. S. Höche, F. Krauss, M. Schönherr and F. Siegert, JHEP **1209** (2012) 049.
- [26] F. Cascioli, P. Maierhöfer and S. Pozzorini, Phys. Rev. Lett. **108**, 111601 (2012); G. Ossola, C. G. Papadopoulos and R. Pittau, JHEP **0803**, 042 (2008). A. van Hameren, Comput. Phys. Commun. **182**, 2427 (2011).
- [27] S. Frixione and B. R. Webber, JHEP **0206**, 029 (2002).
- [28] A. Djouadi, J. Kalinowski and M. Spira, Comput. Phys. Commun. **108**, 56 (1998).
- [29] P. Artoisenet, R. Frederix, O. Mattelaer and R. Rietkerk, JHEP **1303**, 015 (2013).
- [30] S. Hche, S. Kuttimalai, S. Schumann and F. Siegert, Eur. Phys. J. C **75**, no. 3, 135 (2015).
- [31] M. Cacciari, G. P. Salam and G. Soyez, JHEP **0804**, 063 (2008); M. Cacciari, G. P. Salam and G. Soyez, Eur. Phys. J. C **72**, 1896 (2012).
- [32] G. Aad *et al.* [ATLAS Collaboration], JHEP **1205**, 128 (2012).
- [33] CMS Collaboration [CMS Collaboration], CMS-PAS-BTV-13-001.
- [34] D. Alves *et al.* [LHC New Physics Working Group Collaboration], J. Phys. G **39**, 105005 (2012).
- [35] J. F. Gunion, H. E. Haber, G. L. Kane and S. Dawson, Front. Phys. **80**, 1 (2000).
- [36] G. C. Branco, P. M. Ferreira, L. Lavoura, M. N. Rebelo, M. Sher and J. P. Silva, Phys. Rept. **516**, 1 (2012).
- [37] B. Coleppa, F. Kling and S. Su, JHEP **1401**, 161 (2014); O. Eberhardt, U. Nierste and M. Wiebusch, JHEP **1307**, 118 (2013); A. Celis, V. Ilisie and A. Pich, JHEP **1307**, 053 (2013); JHEP **1312**, 095 (2013).
- [38] J. Bernon, J. F. Gunion, H. E. Haber, Y. Jiang and S. Kraml, Phys. Rev. D **92**, no. 7, 075004 (2015).
- [39] J. Bernon, J. F. Gunion, H. E. Haber, Y. Jiang and S. Kraml, Phys. Rev. D **93**, no. 3, 035027 (2016).
- [40] Examples of recent work on the topic are N. Craig, J. Galloway and S. Thomas, arXiv:1305.2424 [hep-ph]; R. V. Harlander, S. Liebler and T. Zirke, JHEP **1402**, 023 (2014); S. Kanemura, K. Tsumura, K. Yagyu and H. Yokoya, Phys. Rev. D **90**, 075001 (2014); B. Hespel, D. Lopez-Val and E. Vryonidou, JHEP **1409**, 124 (2014); S. von Buddenbrock *et al.*, arXiv:1606.01674 [hep-ph].
- [41] Cf. among others J. F. Gunion and H. E. Haber, Phys. Rev. D **72**, 095002 (2005); E. Ma, Phys. Rev. D **73**, 077301 (2006); G. C. Dorsch, S. J. Huber, K. Mimasu and J. M. No, Phys. Rev. Lett. **113**, no. 21, 211802 (2014); N. Blinov, S. Profumo and T. Stefaniak, JCAP **1507**, no. 07, 028 (2015); J. O. Gong, H. M. Lee and S. K. Kang, JHEP **1204**, 128 (2012); A. Ilnicka, M. Krawczyk and T. Robens, Phys. Rev. D **93**, no. 5, 055026 (2016);
- [42] Cf. e.g. M. Carena and H. E. Haber, Prog. Part. Nucl. Phys. **50**, 63 (2003); J. Hetzel and B. Stech, Phys. Rev. D **91**, 055026 (2015); D. B. Kaplan, H. Georgi and S. Dimopoulos, Phys. Lett. B **136**, 187 (1984); K. Agashe, R. Contino and A. Pomarol, Nucl. Phys. B **719**, 165 (2005); M. Schmaltz and D. Tucker-Smith, Ann. Rev. Nucl. Part. Sci. **55**, 229 (2005);
- [43] M. Carena, I. Low, N. R. Shah and C. E. M. Wagner, JHEP **1404**, 015 (2014).
- [44] A. Delgado, G. Nardini and M. Quiros, JHEP **1307**, 054 (2013).
- [45] G. Belanger, B. Dumont, U. Ellwanger, J. F. Gunion and S. Kraml, Phys. Rev. D **88**, 075008 (2013).
- [46] D. Lopez-Val, T. Plehn and M. Rauch, JHEP **1310**, 134 (2013).
- [47] T. Robens and T. Stefaniak, Eur. Phys. J. C **76**, no. 5, 268 (2016); F. Bojarski, G. Chalons, D. Lopez-Val and T. Robens, JHEP **1602**, 147 (2016).
- [48] G. D’Ambrosio, G. F. Giudice, G. Isidori and A. Strumia, Nucl. Phys. B **645**, 155 (2002); A. Dery, A. Efrati, G. Hiller, Y. Hochberg and Y. Nir, JHEP **1308**, 006 (2013).
- [49] A. Pich and P. Tuzon, Phys. Rev. D **80**, 091702 (2009).
- [50] Y. Bai, V. Barger, L. L. Everett and G. Shaughnessy, Phys. Rev. D **87**, 115013 (2013).
- [51] D. Eriksson, J. Rathsmann and O. Stal, Comput. Phys. Commun. **181**, 189 (2010).
- [52] P. Bechtle, O. Brein, S. Heinemeyer, G. Weiglein and K. E. Williams, Comput. Phys. Commun. **181**, 138 (2010); P. Bechtle, O. Brein, S. Heinemeyer, G. Weiglein and K. E. Williams, Comput. Phys. Commun. **182**, 2605 (2011).
- [53] F. Mahmoudi, Comput. Phys. Commun. **178**, 745 (2008); Comput. Phys. Commun. **180**, 1718 (2009).
- [54] P. Bechtle, S. Heinemeyer, O. Stal, T. Stefaniak and G. Weiglein, Eur. Phys. J. C **74**, no. 2, 2711 (2014); O. Stal and T. Stefaniak, PoS EPS **-HEP2013**, 314 (2013).
- [55] F. Kling, J. M. No and S. Su, arXiv:1604.01406 [hep-ph].
- [56] D. Toussaint, Phys. Rev. D **18**, 1626 (1978); J. M. Frere and J. A. M. Vermaseren, Z. Phys. C **19**, 63 (1983); S. Bertolini, Nucl. Phys. B **272**, 77 (1986); W. Hollik, Z. Phys. C **32**, 291 (1986); W. Hollik, Z. Phys. C **37**, 569 (1988); C. D. Froggatt, R. G. Moorhouse and I. G. Knowles, Phys. Rev. D **45**, 2471 (1992); W. Grimus, L. Lavoura, O. M. Ogreid and P. Osland, J. Phys. G **35**, 075001 (2008); Nucl. Phys. B **801**, 81 (2008).
- [57] M. Baak *et al.* [Gfitter Group Collaboration], Eur. Phys. J. C **74**, 3046 (2014).
- [58] A. G. Akeroyd, A. Arhrib and E. M. Naimi, Phys. Lett. B **490**, 119 (2000); S. Kanemura, T. Kubota and E. Takasugi, Phys. Lett. B **313**, 155 (1993); J. Maalampi, J. Sirkka and I. Vilja, Phys. Lett. B **265**, 371 (1991);

- I. F. Ginzburg and I. P. Ivanov, Phys. Rev. D **72**, 115010 (2005); P. Osland, P. N. Pandita and L. Selbuz, Phys. Rev. D **78**, 015003 (2008).
- [59] J. F. Gunion and H. E. Haber, Phys. Rev. D **67**, 075019 (2003).
- [60] C. Y. Chen and S. Dawson, Phys. Rev. D **87**, 055016 (2013).
- [61] S. Kanemura, T. Kasai and Y. Okada, Phys. Lett. B **471**, 182 (1999); B. M. Kastening, hep-ph/9307224; J. Velhinho, R. Santos and A. Barroso, Phys. Lett. B **322**, 213 (1994); S. Nie and M. Sher, Phys. Lett. B **449**, 89 (1999); P. M. Ferreira, R. Santos and A. Barroso, Phys. Lett. B **603**, 219 (2004); Erratum: [Phys. Lett. B **629**, 114 (2005)]; M. Maniatis, A. von Manteuffel, O. Nachtmann and F. Nagel, Eur. Phys. J. C **48**, 805 (2006); P. M. Ferreira and D. R. T. Jones, JHEP **0908**, 069 (2009).
- [62] J. Abdallah *et al.* [DELPHI Collaboration], Eur. Phys. J. C **34**, 399 (2004); G. Abbiendi *et al.* [ALEPH and DELPHI and L3 and OPAL and LEP Collaborations], Eur. Phys. J. C **73**, 2463 (2013); CMS Collaboration [CMS Collaboration], CMS-PAS-HIG-14-020; V. Khachatryan *et al.* [CMS Collaboration], JHEP **1511**, 018 (2015); B. Coleppa, F. Kling and S. Su, JHEP **1412**, 148 (2014).
- [63] G. Aad *et al.* [ATLAS Collaboration], Phys. Rev. Lett. **113**, no. 17, 171801 (2014).
- [64] G. Aad *et al.* [ATLAS Collaboration], JHEP **1411**, 056 (2014).
- [65] V. Khachatryan *et al.* [CMS Collaboration], JHEP **1410**, 160 (2014).
- [66] CMS Collaboration [CMS Collaboration], CMS-PAS-HIG-14-029.
- [67] CMS Collaboration [CMS Collaboration], CMS-PAS-HIG-12-025.
- [68] S. Schael *et al.* [ALEPH and DELPHI and L3 and OPAL and LEP Working Group for Higgs Boson Searches Collaborations], Eur. Phys. J. C **47**, 547 (2006).
- [69] J. Ellis, D. S. Hwang, K. Sakurai and M. Takeuchi, JHEP **1404**, 004 (2014) doi:10.1007/JHEP04(2014)004 [arXiv:1312.5736 [hep-ph]].
- [70] F. Boudjema, R. M. Godbole, D. Guadagnoli and K. A. Mohan, Phys. Rev. D **92**, no. 1, 015019 (2015) doi:10.1103/PhysRevD.92.015019 [arXiv:1501.03157 [hep-ph]].
- [71] J. Chang, K. Cheung, J. S. Lee and C. T. Lu, arXiv:1607.06566 [hep-ph].
- [72] F. Demartin, F. Maltoni, K. Mawatari, B. Page and M. Zaro, Eur. Phys. J. C **74**, no. 9, 3065 (2014) doi:10.1140/epjc/s10052-014-3065-2 [arXiv:1407.5089 [hep-ph]].
- [73] G. Mahlon and S. J. Parke, Phys. Rev. D **53**, 4886 (1996) [hep-ph/9512264]. C. R. Schmidt and M. E. Peskin, Phys. Rev. Lett. **69**, 410 (1992).
- [74] V. Khachatryan *et al.* [CMS Collaboration], Phys. Lett. B **750**, 494 (2015).
- [75] J. Abdallah *et al.* [DELPHI Collaboration], Eur. Phys. J. C **38**, 1 (2004).
- [76] B. Aubert *et al.* [BaBar Collaboration], Phys. Rev. D **77**, 051103 (2008); S. Su and B. Thomas, Phys. Rev. D **79**, 095014 (2009); M. Aoki, S. Kanemura, K. Tsumura and K. Yagyu, Phys. Rev. D **80**, 015017 (2009); F. Mahmoudi and T. Hurth, PoS ICHEP **2012**, 324 (2013); Y. Amhis *et al.* [Heavy Flavor Averaging Group (HFAG) Collaboration], arXiv:1412.7515 [hep-ex]; M. Misiak *et al.*, Phys. Rev. Lett. **114**.
- [77] D. Goncalves, F. Krauss and R. Linten, Phys. Rev. D **93**, no. 5, 053013 (2016) doi:10.1103/PhysRevD.93.053013 [arXiv:1512.05265 [hep-ph]].
- [78] G. Aad *et al.* [ATLAS Collaboration], Eur. Phys. J. C **75**, no. 7, 349 (2015) doi:10.1140/epjc/s10052-015-3543-1 [arXiv:1503.05066 [hep-ex]]. V. Khachatryan *et al.* [CMS Collaboration], Eur. Phys. J. C **75**, no. 6, 251 (2015) doi:10.1140/epjc/s10052-015-3454-1 [arXiv:1502.02485 [hep-ex]].